

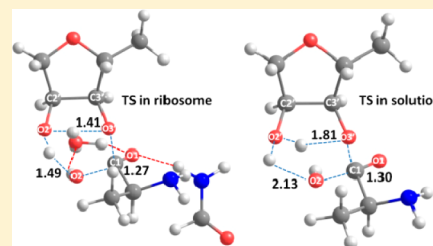
Quantum Mechanical Study on the Mechanism of Peptide Release in the Ribosome

Carles Acosta-Silva, Joan Bertran,* Vicenç Branchadell, and Antoni Oliva

Departament de Química, Universitat Autònoma de Barcelona, 08193 Bellaterra, Spain

S Supporting Information

ABSTRACT: A quantum mechanical study of different concerted mechanisms of peptide release in the ribosome has been carried out using the M06-2X density functional. Reoptimization with MP2 has also been carried out for the stationary points of some selected mechanisms. The uncatalyzed processes in solution have been treated with the SMD solvation model. We conclude that the 2'-OH plays an important catalytic role and that it takes place via a zwitterionic transition state, this TS being stabilized by the presence of oxyanion holes or by the solvent. The comparison with our previous study on the peptide bond formation shows that both processes proceed via two different mechanisms, in such a way that the TS of the aminolysis has an ion-pair instead of a zwitterionic character. So, despite the limitations of the model we have used, we can conclude that there is catalytic promiscuity at the peptidyl transferase center (PTC) of the ribosome.



INTRODUCTION

The active site of the ribosome, the peptidyl transferase center (PTC), catalyzes two chemical reactions during protein synthesis. In the first reaction, peptide bonds are formed by the nucleophilic attack of an aminoacyl-tRNA in the A-site on peptidyl t-RNA in the P-site. In the second reaction, water acts as the nucleophile in the hydrolysis of the peptidyl t-RNA.^{1,2} Hydrolysis of the ester link of the peptidyl-tRNA is stimulated normally by the binding of release factors (RFs). However, an unacylated tRNA or just the trinucleotide CCA binding to the ribosomal A-site can also stimulate deacylation.^{3,4} It is then obvious that there is at least substrate promiscuity, since there are two different nucleophiles, but is it also a catalytic promiscuity?^{5–9} Although both substrates are nucleophiles, the amino group has a bigger nucleophilic character than water. In contrast, water is a better proton donor than the amino group, so that the mechanisms can be quite different. This is the first issue that will be addressed in this paper.

Translation termination is mediated by two classes of peptide release factors (RFs), the first RF having been isolated by Capecchi¹⁰ in 1967. Class I RFs directly decode the stop codon and catalyze the hydrolysis of the peptidyl-t-RNA ester bond. In prokaryotes, RF1 and RF2 possess overlapping codon specificities, recognizing UAA/UAG and UAA/UGA, respectively. Eukaryotic eRF1 is able to recognize all three stop codons, namely, UAA, UAG, and UGA.^{11–19} Prokaryotic and eukaryotic class I RFs share one motif: a GGQ tripeptide positioned in a loop at the end of a stem region that interacts with the ribosomal PTC, the glutamine side chain being specifically methylated.^{20–26} It has been assumed that this motif triggers peptidyl-tRNA hydrolysis. Unlike the extended structure of eRF1, the crystal structures of isolated RF1 and RF2 are in a compact form, in such a way that the distance between GGQ and the anticodon is about 25 Å, while in the

ribosome the distance between the decoding center (DC) and the PTC is around 73 Å. This seems to indicate that the anticodon and GGQ motifs cannot be both at DC and PTC simultaneously. This apparent paradox can be solved if one takes into account that ribosome-bound RF1 and RF2 adopt an “open” conformation.^{27–35} SAXS experiments showed that RF1 adopts a similar “open” conformation in solution.³⁶ On the other hand, similar experiments suggest that RF2 keeps the compact conformation in solution.³⁷ The role of RFs in codon recognition has encouraged the idea that these proteins may mimic tRNA molecules both in size and in shape, in such a way that they may produce identical conformational changes in the ribosome.^{2,28,30,33} Class II release factors (RF3 in prokaryotes and eRF3 in eukaryotes) are GTPases with limited homology that is restricted to their GTP-binding domain. RF3 and eRF3 have entirely different functions in the termination process.^{38–43}

Several works^{1,2,12,22,44–53} have been devoted to analyze the mechanism by which the GGQ motif triggers peptidyl-tRNA hydrolysis. Song et al.¹² suggested that the glutamine residue coordinates a water molecule to mediate the hydrolytic activity at the PTC. This suggestion was questioned by other authors,^{22,44} since mutations of the glutamine residue are not highly deleterious to the hydrolysis reaction when compared to mutations of the two glycines.^{22,27,44–46} However, it has been reported that the methylated amino acid Q of the RF1 GGQ motif is critical for the observed specificity of water as the nucleophile. These data lead to a model where RFs make two distinct contributions to catalysis: a relatively nonspecific activation of the catalytic center and a specific selection of

Received: November 7, 2012

Revised: February 26, 2013

Published: February 27, 2013

water as a nucleophile.⁴⁶ The high-resolution structures of class I RFs bound to bacterial ribosome were determined by the groups of Ramakrishnan⁴⁷ and Noller^{48,49} in 2008, considerably advancing our understanding on the mechanism of prokaryotic translation termination.⁵⁰ All three structures showed that the conserved GGQ motif is positioned in the PTC. Two Gly residues in the GGQ motif adopt conformations that are not possible for other amino acids, explaining the drastic reduction in the activity of RFs when they are mutated. The two above-mentioned groups proposed different mechanisms for the hydrolysis reaction. According to the Ramakrishnan lab, the glutamine adopts a conformation in which the side chain accommodates a water molecule in the PTC, hydrogen bonded to the backbone amide of the glutamine residue.^{1,45,47,51} On the other hand, Noller's group proposes that the main-chain amide of the glutamine is positioned to participate in the catalysis by forming a hydrogen bond with the leaving 3' OH group and/or with the transition state oxyanion.^{45,48,49,52,53} The reason for this discrepancy lies in the fact that while both groups find a similar structure in which the glutamine side chain points away from the ribose, the group of Ramakrishnan argues that there exists an alternative conformation which seems to predominate. In this alternative conformation the side-chain carbonyl hydrogen-bonds to the ribose of A76 in P-site tRNA.⁴⁷

It has also been found that substitution of A2602 with C or its deletion abolishes the ribosome's ability to promote peptide release, but it has little effect on transpeptidation. This seems to indicate that the mechanism of peptide release is distinct from that of peptide bond formation.^{54,55} Although the role of A2602 is not yet clear, it probably helps to stabilize the GGQ loop in a catalytically active conformation.^{51,56} Brunelle et al.⁵⁷ have shown that the 2'-OH of the P-site tRNA substrate plays a critical role in the peptide release reaction catalyzed by class I release factors on the bacterial ribosome. These observations parallel earlier studies⁵⁸ of the mechanism of the peptidyl transfer reaction and argue that related mechanisms are at the heart of catalysis for these reactions. However, a recent work⁵⁹ has confirmed the important role of the 2'-OH in the release reaction, but it has dramatically decreased its importance in the peptidyl transfer reaction, this fact suggesting that there might be mechanistic differences between both reactions.

From a theoretical point of view, Trobro and Aqvist^{60–62} have studied the ribosomal peptidyl transfer reaction by carrying out extensive molecular dynamics (MD) free energy calculations with Warshel's empirical valence bond (EVB) method.⁶³ Using the same methodology, they have also studied the mechanism of the peptide release process.^{64,65} They found that the methylated glutamine residue of the universally conserved GGQ motif plays a key role in the hydrolysis reaction by orienting the water nucleophile and by stabilizing the transition state. Two additional water molecules interacting with the P-site substrate are also found to be critically important. Furthermore, the 2'-OH group of the peptidyl-tRNA substrate is predicted to act as a proton shuttle for the leaving group in analogy with the consensus mechanism for peptidyl transfer. Thus, the ribosome's ability to catalyze both the termination (hydrolysis) and peptidyl transfer (aminolysis) reactions is largely explained by this type of unified mechanism, with similar transition states occurring in both processes.

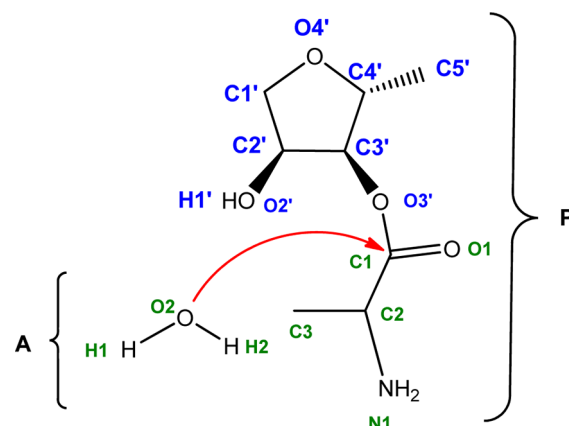
While there have been several quantum-mechanical (QM) studies^{66–72} on the peptidyl transfer reaction, no QM works have been devoted, to our knowledge, to the peptide release process. The studies on the peptidyl transfer reaction have

treated the concerted mechanism and a two-step mechanism with a neutral intermediate, using different methods and different basis sets. In a more recent paper⁷³ we carried out a complete study of the proposed mechanisms using a more recent DFT functional and a larger basis set. The purpose of the present work is to carry out a similar study of the concerted mechanism of the peptide release reaction. The use of the same methodology will permit clarification of whether the mechanisms and the transition state structures of both processes are similar or not.

■ COMPUTATIONAL METHODS

The quantum-mechanical study of a complex system implies the use of a reduced model. Scheme 1 shows the model which

Scheme 1. Schematic Drawing Showing the Reactants in the Nucleophilic Attack of a Water Molecule at A-Site on the Carbonyl Group of the Ester Formed between the Peptide Chain and tRNA at P-Site^a



^aThe numbering of the atoms will be used throughout the paper.

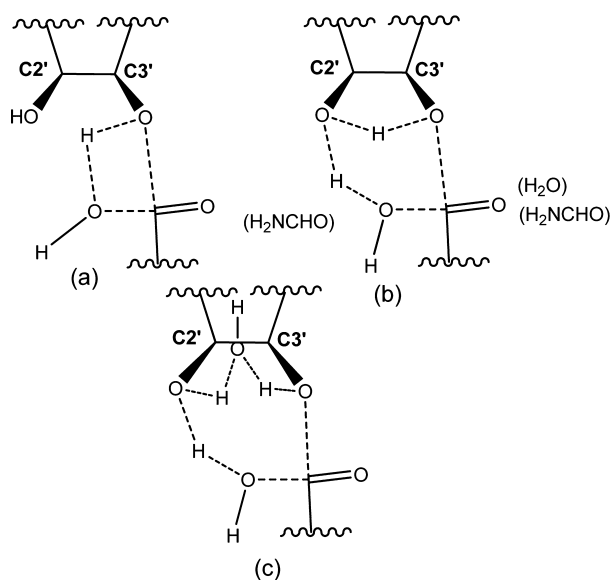
has been adopted in this work. As mentioned in the Introduction we have used the same model previously employed in the study of the peptidyl transfer reaction⁷³ with the obvious exception of the nucleophile. It has to be emphasized that the model we used in that work for the P-site was very similar to the ones adopted in the QM studies carried out by the groups of Yonath,^{68,69} Aqvist,⁷¹ and Liu.⁷² Scheme 1 shows that our model includes all the atoms that intervene in the different possible mechanisms. The main simplifications we did can be summarized as follows. The atom C5', which in the real system is bonded to the oxygen atom of a phosphate in the RNA main chain, has been represented by a methyl group. The base bonded to the C1' has been modeled by a hydrogen atom. The methyl group C3 acts as a model of the lateral chain of an amino acid. In the amino group N1 one of the hydrogen atoms takes the place of a polypeptide chain. Only the three hydrogen atoms which intervene in the process are explicitly shown and numerated.

As it has been mentioned in the Introduction, X-ray data show that the amide groups present in the lateral^{47,51} or in the main chain^{48,49,52} of glutamine in the GGQ motif play an important role in the enzymatic process. Furthermore, MD studies^{64,65} indicate that additional water molecules can also be relevant. So, additional water and/or formamide molecules have been explicitly considered in the philosophy of the theozymes (theoretical enzymes) proposed by Tantillo et al.⁷⁴

The group of Houk carried out^{75,76} theoretical studies of several enzymatic processes, and they have obtained transition structures without any constraint, which are quite close to the X-ray transition state analogues. This structural agreement between the theozyme and the real enzyme is in accord with the paradigm wherein the enzyme structure assumes maximum free energy lowering of the transition state.

Scheme 2 shows the three different mechanisms we have considered for the concerted process. In the first one (a), the

Scheme 2. Transition States of the Proposed Concerted Mechanisms^a



^a(a) Four-membered ring cycle. (b) Six-membered ring cycle. (c) Eight-membered ring cycle.

proton of the water molecule is transferred directly to the leaving group via a four-membered ring cycle. In the second one (b), the transfer is done through the hydroxyl group of sugar via a six-membered ring cycle. In this case, the intervention of additional water and/or formamide molecules has also been considered. Finally, in the third mechanism (c), there is an eight-membered ring cycle due to the intervention of an additional water molecule. As for the peptide release process, there is a lack of experimental and theoretical information about transition state geometries. For this reason, we started from structures which were similar to the four-, six-, and eight-membered rings of the transition states of the peptidyl transfer process to locate and fully characterize (one imaginary frequency) the transition structures of the peptide release reaction. It has to be emphasized that this strategy could favor the similarity between both mechanisms, thus enhancing in this way the importance of discrepancies. For each transition state the intrinsic reaction coordinate⁷⁷ (IRC) was calculated. The final points of each reaction path were used to fully characterize the reactant and product complexes associated with each transition state through a complete optimization. Finally the isolated reactants and products were also optimized. It is worth mentioning that no constraints have been used in any step of our study.

The calculations have been carried out using the M06-2X functional proposed by Truhlar's group,^{78,79} a highly parametrized metahybrid method which has shown to be very

adequate for the study of noncovalent interactions and, especially, hydrogen bonds. Reoptimization with MP2 has also been carried out for the stationary points of some selected mechanisms. All the calculations have been done using the triple- ζ 6-311+G(d,p) basis set. Truhlar^{80–82} has shown that this basis set is very adequate when using the M06-2X functional and that the inclusion of additional diffuse functions is not necessary.

The introduction of the solvent effect has been carried out using the SMD method of Marenich et al.⁸³ SMD is a universal solvation model, where “universal” denotes its applicability to any charged or uncharged solute in any solvent or liquid medium for which a few key descriptors are known. In SMD, “D” stands for “density” to denote that the full solute electron density is used without defining partial atomic charges, as it was the case in the previous SM8 method.⁸⁴ The SMD model separates the observable solvation free energy into two components: the long-range bulk electrostatic contribution arising from a self-consistent reaction field treatment that involves the solution of the nonhomogeneous Poisson equation for electrostatics in terms of the integral equation-formalism polarizable continuum model, and the cavity-dispersion-solvent-structure term, which arises from short-range interactions between the solute and solvent molecules in the first solvation shell.

Thermochemical corrections to the energy values have been computed using the standard rigid rotor/harmonic oscillator formulas.⁸⁵ Relative Gibbs energies in solution have been computed using as the reference state 1 mol L^{−1} at a temperature of 298.15 K.

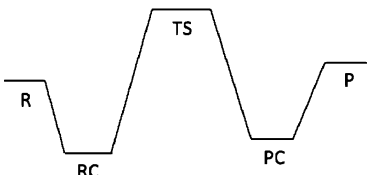
All quantum-mechanical calculations have been performed through the Gaussian 09 package,⁸⁶ and the stationary points have been fully characterized. Full Natural Bond Orbital Analysis has been carried out with NBO version 3.⁸⁷

RESULTS

As stated in the Introduction, we have studied different concerted mechanisms for the peptide release process in the ribosome and in solution. In each case, the energy values, the geometry parameters of the stationary points, and the charge distribution will be successively analyzed.

In the Ribosome. Table 1 shows the variation with respect to the isolated reactants (R) of the potential energy, the enthalpy, and the Gibbs free energy corresponding to the reactant complex (RC), the transition state (TS), the product complex (PC), and the isolated products (P) for each one of the nine studied mechanisms. The first three mechanisms are those depicted in Scheme 2 and proceed via a four-membered ring cycle (Scheme 2a), a six-membered ring cycle (Scheme 2b), or an eight-membered ring cycle (Scheme 2c). These mechanisms will be hereafter named I-4, I-6, and I-8, respectively. In these three cases the M06-2X stationary points have been reoptimized at the MP2 level. One can observe that the relative energies obtained with MP2 are quite similar to the M06-2X ones, thus confirming that the choice of this functional was adequate. For the six-membered ring cycle, six additional mechanisms have been considered through the inclusion of one or two molecules of water (w) or formamide (f). When a water molecule is added (mechanisms I-6w1 and I-6w2), it is hydrogen bonded to the carbonyl oxygen atom, the difference between both mechanisms being that in the first case the water molecule acts also as an acceptor of a hydrogen atom of the nucleophile. In the mechanisms I-6f1 and I-6f2, it is a

Table 1. Variation with Respect to the Isolated Reactants (R) of the Potential Energy, the Enthalpy, and the Gibbs Free Energy of the Reactant Complex (RC), the Transition State (TS), the Product Complex (PC), and the Isolated Products (P) for Each One of the Nine Studied Mechanisms^a



mechanism	energy	R	RC	TS	PC	P
I-4	ΔE	0.0 (0.0)	-8.7 (-8.1)	45.0 (43.9)	1.6 (1.2)	7.5 (10.1)
	ΔH	0.0 (0.0)	-6.9 (-6.5)	43.3 (41.8)	0.6 (3.1)	8.3 (10.8)
	ΔG	0.0 (0.0)	2.5 (1.9)	55.4 (53.3)	10.5 (11.4)	6.8 (9.1)
I-6	ΔE	0.0 (0.0)	-8.7 (-8.1)	39.2 (39.5)	-4.4 (-3.2)	1.2 (3.7)
	ΔH	0.0 (0.0)	-6.9 (-6.5)	37.5 (36.8)	-2.0 (-1.0)	1.9 (4.5)
	ΔG	0.0 (0.0)	2.6 (1.9)	51.4 (50.3)	7.6 (7.1)	0.1 (2.7)
I-8	ΔE	0.0 (0.0)	-9.5 (-9.3)	32.1 (33.7)	-9.5 (-7.8)	4.2 (6.2)
	ΔH	0.0 (0.0)	-7.2 (-7.8)	30.8 (32.4)	-7.1 (-5.7)	5.22 (6.8)
	ΔG	0.0 (0.0)	3.4 (0.3)	45.6 (47.9)	2.7 (4.8)	3.7 (5.6)
I-6w1	ΔE	0.0	-11.4	30.5	-15.5	-5.6
	ΔH	0.0	-9.4	29.2	-12.9	-4.2
	ΔG	0.0	0.7	43.9	-1.8	-5.2
I-6w2	ΔE	0.0	-9.7	35.3	-6.8	3.0
	ΔH	0.0	-8.0	34.0	-4.8	3.5
	ΔG	0.0	1.1	48.8	5.5	0.7
I-6f1	ΔE	0.0	-10.5	40.1	-3.12	2.3
	ΔH	0.0	-8.7	38.5	-1.2	3.0
	ΔG	0.0	1.2	52.6	8.0	0.6
I-6f2	ΔE	0.0	-13.6	30.3	-14.8	-4.9
	ΔH	0.0	-11.5	28.6	-12.3	-4.0
	ΔG	0.0	-0.2	45.1	0.1	-3.2
I-6wf	ΔE	0.0	-7.8	32.0	-20.3	-1.8
	ΔH	0.0	-6.1	30.8	-17.8	-1.0
	ΔG	0.0	2.4	43.5	-6.3	-3.4
I-6ff	ΔE	0.0	-17.4	27.2	-22.4	-5.0
	ΔH	0.0	-15.3	25.9	-20.4	-4.0
	ΔG	0.0	-3.5	40.2	-7.4	-6.4

^aResults in kcal mol⁻¹. In parentheses, MP2 results.

formamide molecule which is hydrogen bonded to the carbonyl oxygen atom or to the nucleophile, respectively. Finally, the carbonyl oxygen atom has been hydrogen bonded to a water molecule and a formamide molecule (mechanism I-6wf) and also to two formamide molecules (mechanism I-6ff).

Regarding the energy barriers of the bimolecular processes, it can be observed that the one of mechanism I-6 (39.2 kcal mol⁻¹ at the M06-2X level) is 5.8 kcal mol⁻¹ lower than that of mechanism I-4 (45.0 kcal mol⁻¹), thus implying that the substrate assisted catalysis favors the process. The inclusion of one water molecule to permit the formation of an eight-

membered ring cycle (mechanism I-8) leads to an energy barrier of 32.1 kcal mol⁻¹, which is 7.1 kcal mol⁻¹ lower than the one of the six-membered cycle (and thus 12.9 kcal mol⁻¹ with respect to the four-membered one). So, it is clear that the addition of a water molecule makes the process more favorable. A similar conclusion can be reached when the water molecule is placed in the two other positions we have studied (mechanisms I-6w1 and I-6w2), although in the last case the decrease of the energy barrier is smaller. The inclusion of a formamide molecule in the six-membered ring process does not favor the catalysis when it is hydrogen bonded to the carbonyl oxygen atom (mechanism I-6f1) while the energy barrier is lowered to 30.3 kcal mol⁻¹ when it is hydrogen bonded to the nucleophile (mechanism I-6f2). The simultaneous addition of water and formamide leads to an energy barrier of 32.0 kcal mol⁻¹, which is very similar to the value obtained for mechanisms I-8 and I-6w1. Finally, the addition of two formamide molecules (mechanism I-6ff) leads to the smallest energy barrier we have obtained (27.2 kcal mol⁻¹). The activation enthalpies are very similar to the energy barriers, their values being slightly smaller (less than 2 kcal mol⁻¹ in all cases). The Gibbs free energy barriers are 12–17 kcal mol⁻¹ higher than the enthalpy ones, in good agreement with the expected negative value of the entropy terms. However, it has to be emphasized that a big part of this increase (between 8.5 and 11.8 kcal mol⁻¹) comes from the formation of the reactant complex which implies the conversion of 6 translational and rotational degrees of freedom into vibrations and pseudorotations. The high value of the entropy term provokes that the free energy of the reactant complex is usually higher than that of the isolated reactants, in such a way that this complex would not be formed. This can be surprising since the reactant complex is expected to play the role of the Michaelis complex which, as it is well-known, is thermodynamically stable. As we have used a simplified model, our results support the idea that the real ribosome acts as an entropic trap.⁸⁸ In a similar way, the Gibbs energy of the product complex is generally higher than that of the isolated products.

Figures 1 and 2 present the geometries of the transition structures corresponding to the nine mechanisms considered in Table 1. There are four bond lengths which play an important role in all the studied mechanisms: the breaking of the O2–H1 and C1–O3' bonds and the formation of the O2–C1 and O3'–H bonds (see Scheme 1 for the numbering of atoms). Let us first present the results corresponding to mechanisms I-4, I-6, and I-8 (Figure 1). In mechanism I-4, H1 is directly transferred from O2 to O3', the distances O2–H1 and O3'–H1 being the same in the transition state. The other two distances of the cycle (C1–O3' and C1–O2) are also quite similar. At the MP2 level, the two distances corresponding to the hydrogen transfer are almost identical to the DFT results, whereas the other two distances are slightly larger. In mechanism I-6, the hydrogen transfer from O2 to O3' occurs via the hydroxyl group of the sugar, in such a way that H1 is transferred from O2 to O2' and H1' is transferred from O2' to O3', the first transfer being much more advanced in the TS. This TS is quite similar at the MP2 level, although the bond distances indicate that the H1 is slightly less transferred than in the DFT results while the contrary occurs in the transfer of H1'. Regarding mechanism I-8, the H1 transfer is almost completely done as it is the formation of the C1–O2 bond, while the other two hydrogen transfers are at an initial stage and the C1–O3' bond is almost completely broken. These results are confirmed at the MP2

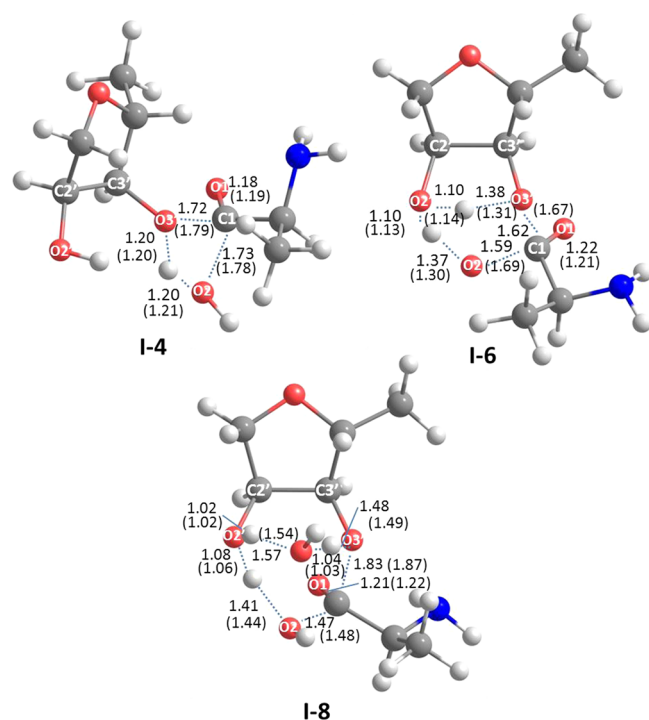


Figure 1. Geometries of the transition states corresponding to mechanisms I-4, I-6, and I-8. Selected distances in Å. In parentheses, MP2 distances.

level. It is worth mentioning that the transition vector has a quite low frequency value (around 300 cm^{-1}). Regarding the other six mechanisms (Figure 2), they are in fact variations from the I-6 one, the six-membered ring being conserved in all of them. For mechanisms I-6w1, I-6w2, I-6f1, I-6wf, and I-6ff, one or two molecules of water or formamide are hydrogen-bonded to O1. The transition states of these five mechanisms are quite similar to the I-6 one, a hydrogen transfer being much more advanced than the other one. One can also observe that in mechanisms I-6w1 and I-6wf the water molecule acts also as a hydrogen acceptor, thus implying some cooperative effect. This cooperative effect is also observed in mechanism I-6ff, one of the formamide molecules playing now the bifunctional role. Finally, in mechanism I-6f2 the carbonyl oxygen atom of the formamide molecule is hydrogen bonded to O2, this hydrogen bond being quite strong, since the O2–H bond length has increased from 0.97 Å in the RC to 0.99 Å , while the distance between this hydrogen atom and the O of formamide has decreased from 2.07 Å to 1.73 Å . The existence of this strong hydrogen bond leads to a decrease of the O2–C1 distance from 1.59 Å in mechanism I-6 to 1.51 Å in mechanism I-6f2, thus showing the increase of the nucleophilic character of water.

Let us analyze the C1–O1 bond, whose lengths at the transition states are presented in Figures 1 and 2. The shortest value of this bond length corresponds to mechanism I-4 (1.18 Å). The bond length increases to 1.22 Å for mechanisms I-6 and I-8, the increase being related to the formation of an oxyanion and the corresponding decrease of the CO double bond character. The inclusion of one or two molecules of water or formamide in the other six mechanisms leads to a new increase of the C1–O1 bond length, this increase being especially important when both molecules stabilize the oxyanion in mechanisms I-6wf and I-6ff. The trend indicated by this bond length is confirmed by the values of the Wiberg

indexes⁸⁹ shown in Table 2. One can observe that the value corresponding to I-4 (1.79) shows that the C1–O1 has still a clear double bond character (its value in the reactants is around 1.75). As it was to be expected, the Wiberg index diminishes as far as the bond length increases, the smallest values being 1.35 and 1.34 for mechanisms I-6wf and I-6ff, respectively, thus confirming that in these mechanisms the C1–O1 bond has the greatest single bond character, a fact which is a direct consequence of the degree of stabilization of the oxyanion. This increase of single bond character and the simultaneous formation of the C1–O2 bond imply that the C1 atom adopts a tetrahedral arrangement. To confirm this we have computed the sum of the six bond angles around C1 (θ_{C1}), this sum being expected to be 657° in an sp^3 hybridization scheme and 630° when the sp^2 hybridization of the C1 atom is maintained as the attacking or leaving groups are far away. The values of θ are also shown in Table 2. One can observe that the value for mechanism I-4 is intermediate between those of sp^2 and sp^3 hybridizations, while in the other mechanisms the tetrahedral character predominates. Once more, the tetrahedral character reaches its maximum for mechanisms I-6wf and I-6ff. Finally, the values of the C3'–O3'–C1–N2 dihedral angle in the transition structure are presented in the last column of Table 2. Its sign indicates the side of the C3' O3' C1 plane in which the attack is produced. In all the transition structures, this dihedral is negative, thus corresponding to an S chirality. Schmeing et al.⁹⁰ obtained a similar conclusion for the aminolysis reaction from their experimental results.

Table 3 presents the dipole moments, the natural atomic populations over several relevant atoms, and the variations of these atomic populations with respect to the RCs for the transition structures of the nine studied mechanisms. One can observe that the values of the dipole moments are quite variable, its range changing from 2.11 D for mechanism I-6w1 to 7.82 D for I-6f1. The existence of small dipole moments can be explained if one takes into account that the electronic charge transfer from the nucleophile to the substrate is compensated by a proton transfer from the O2 atom of water. In this way the water molecule increases its nucleophilic character. Regarding the natural atomic populations, one can observe that O2 and H1 are losing electrons, these electrons being essentially transferred to O3' and O1. For mechanisms I-4, I-6, and I-8, the MP2 populations follow the same trend, although the negative and positive charges are increased. One can observe that the negative charges and their variations are greater for O1 than for O3', except in mechanisms I-4 and I-8. The reason for these exceptions is that the heterolytic breaking of the C1–O3' bond is much more advanced in these two mechanisms, while the C1–O1 bond keeps an important double bond character. It is worth mentioning that the water molecule in mechanism I-8 stabilizes both the negative charge over O3' and the positive charge of the group around O2' in a cooperative way. So, it accentuates the heterolytic breaking and, thus, the concentration of the negative charge on O3' reaches its maximum value (-0.81). In the other mechanisms, the transition structures have a zwitterionic character, with the formation of an oxyanion around O1. Except in two cases (I-6 and I-6f2), the oxyanion is usually stabilized by the presence of an oxyanion hole (one or two molecules of water or formamide). The positive charge of the zwitterion is concentrated around the O2' atom, which is the one that receives the proton from O2. As it was to be expected, the charge over O1 is maximum (-0.90 and -0.89) for mechanisms I-6wf and I-6ff,

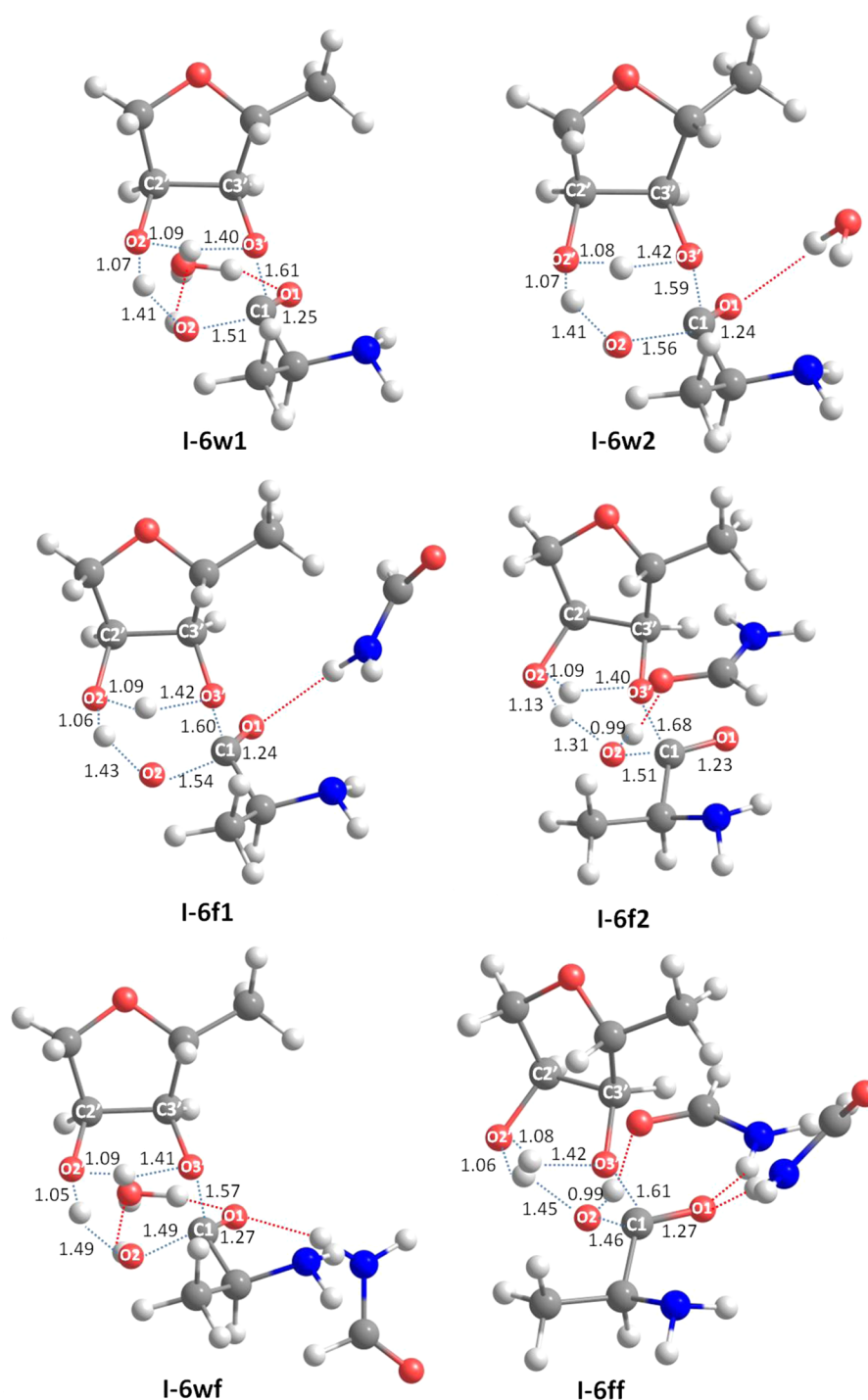


Figure 2. Geometries of the transition states corresponding to mechanisms I-6w1, I-6w2, I-6f1, I-6f2, I-6wf, and I-6ff. Selected distances in Å.

respectively, in which the two additional molecules intervene in the oxyanion hole. The formation of the oxyanion is consistent with the length of the C1–O1 bond and its loss of double bond character, as it has been discussed above.

In Solution (Uncatalyzed Reaction). Table 4 is analogous to Table 1 for the two studied uncatalyzed mechanisms in solution. The two mechanisms take into account the solvent effect of water using the SMD method.⁸³ The energy and enthalpy are indicated as E' and H' , since the computed energy is obtained by adding free energy of solvation to gas-phase potential energy surface. This new E' surface is named, according to statistical mechanics, potential of mean force.⁹¹ In

contrast, G is the real free energy as it contains the free energy of solvation. The starting points for studying the two mechanisms in solution have been the transition state structures of the four- and six-membered ring mechanism in the ribosome (mechanisms I-4 and I-6). The two mechanisms in solution are, thus, called I-4S and I-6S, respectively.

The fact that the free energy of the reactant complexes is higher than that of the reactants (Table 4) had to be expected, as the solvent does not play the role of an entropy trap. In a similar way, the Gibbs energy of the product complex is higher than that of the isolated products. One can also observe that mechanism I-6S is clearly more favorable than I-4S, the barriers

Table 2. C–O Distance (Å), C–O Wiberg Indexes, θ_{C1} , and the C3'–O3'–C1–N2 Dihedral Angle for the Transition Structures of the Nine Studied Mechanisms

mechanism	C1–O1 (distance)	C1–O1 (Wiberg index)	θ_{C1}	$D(C3'-O3'-C1-N2)$
I-4	1.18	1.79	647.2	−114.9
I-6	1.22	1.59	653.9	−79.4
I-8	1.21	1.62	652.4	−105.1
I-6w1	1.25	1.44	654.8	−77.6
I-6w2	1.24	1.51	654.5	−74.3
I-6f1	1.24	1.49	654.5	−81.9
I-6f2	1.23	1.53	654.2	−71.0
I-6wf	1.27	1.35	655.2	−76.6
I-6ff	1.27	1.34	655.3	−69.2

differing by about 10 kcal mol^{−1}. The comparison with the results for the processes in the ribosome (Table 1) shows that there are five mechanisms (I-8, I-6w1, I-6f2, I-6wf, and I-6ff) in which the activation free energies are lower by 3–9 kcal mol^{−1}, in quite good agreement with the value of 6–7 kcal mol^{−1} which can be calculated from the experimental rate constants.^{27,46} In fact, our barriers for the catalyzed reactions are overestimated since, as it has been previously mentioned, the simplified model we have used does not lead to the formation of stable RCs.

Figure 3 shows the geometries of the transition structures of both mechanisms in solution. The dipole moments, the natural atomic populations over selected atoms, and the variation of these atomic populations with respect to the reactant complexes for the transition structures of the two studied mechanisms are presented in Table 5. The comparison with the corresponding mechanisms in the ribosome (Figure 1 and Table 3) shows that I-4S does not present important differences with I-4. One can only mention that the carbonyl C1–O1 double bond is more broken (the Wiberg index being 1.61 instead of 1.79) while the proton transfer and the heterolytic breaking are less advanced than in I-4, in such a way that the charges over O3' and O1 are very similar in the TS of I-4S. On the contrary, the TS of mechanism I-6S greatly differs from the TS of I-6. On one side, the C1–O1 bond presents already a single bond character in the mechanism in solution, in such a way that its Wiberg index is 1.26, while it was 1.59 in mechanism I-6. At the same time, the formation of the C1–O2 bond is more advanced while the C1–O3' bond is less broken

Table 4. Variation with Respect to the Isolated Reactants (R) of the Potential Energy, the Enthalpy, and the Gibbs Free Energy of the Reactant Complex (RC), the Transition State (TS), the Product Complex (PC), and the Isolated Products (P) for Each One of the Two Uncatalyzed Mechanisms^a

mechanism	energy	R	RC	TS	PC	P
I-4S	$\Delta E'$	0.0	−4.8	46.5	−0.6	3.7
	$\Delta H'$	0.0	−2.9	44.9	2.0	4.6
	ΔG	0.0	6.1	55.8	10.6	3.9
	$\Delta E'$	0.0	−4.9	35.8	−3.2	1.8
I-6S	$\Delta H'$	0.0	−2.9	36.8	−0.6	2.7
	ΔG	0.0	5.4	48.8	8.1	1.6

^aResults in kcal mol^{−1}.

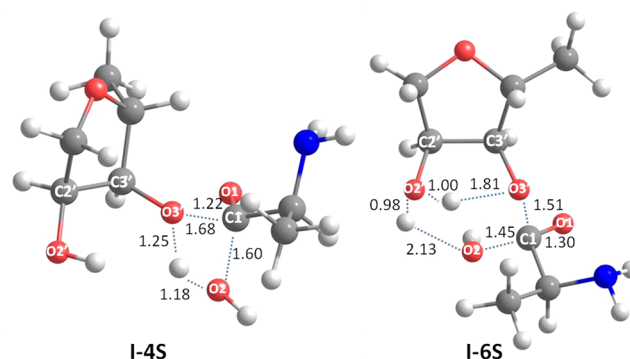


Figure 3. Geometries of the transition states corresponding to the uncatalyzed mechanisms. Selected distances in Å.

in the mechanism in solution. As a direct consequence, one can also observe that the H1 atom is almost completely transferred and that the transfer of the H1' atom is less advanced in solution. Finally, it is worth mentioning that in mechanism I-6S the C1 atom presents its maximum tetrahedral character, with a θ_{C1} angle of 655.9°, very close to the value of 657°

Table 3. Dipole Moments (Debyes), Natural Atomic Populations, and Variations of the Populations with Respect to the RCs for Some Selected Atoms for the Transition Structures of the Nine Studied Mechanisms^a

mechanism	μ	O2	H1	O2'	O3'	O1	O water
I-4	4.74	−0.86	0.10	0.54	0.05	−0.73	0.02
	(5.58)	(−0.92)	(0.03)	(0.56)	(0.07)	(−0.76)	(0.02)
I-6	2.72	−0.87	0.09	0.53	0.05	−0.73	0.02
	(2.08)	(−0.93)	(0.02)	(0.55)	(0.07)	(−0.80)	(−0.02)
I-8	3.38	−0.79	0.17	0.54	0.05	−0.72	0.06
	(3.46)	(−0.83)	(0.14)	(0.57)	(0.07)	(−0.76)	(0.06)
I-6w1	2.11	−0.85	0.13	0.54	0.05	−0.72	0.03
I-6w2	5.75	−0.87	0.09	0.54	0.05	−0.72	0.04
I-6f1	7.82	−0.86	0.11	0.54	0.04	−0.72	0.05
I-6f2	4.33	−0.84	0.15	0.53	0.04	−0.74	0.00
I-6wf	6.98	−0.85	0.14	0.54	0.05	−0.71	0.04
I-6ff	6.00	−0.84	0.16	0.54	0.05	−0.72	0.02

^aIn parentheses, MP2 results.

Table 5. Dipole Moments (Debyes), Natural Atomic Populations, and Variations of the Populations with Respect to the RCs for Some Selected Atoms for the Transition Structures of the Two Uncatalyzed Mechanisms

mechanism	μ	O2		H1		O2'		O3'		O1	
I-4S	7.24	−0.82	0.19	0.56	0.05	−0.78	0.00	−0.75	−0.15	−0.78	−0.10
I-6S	11.67	−0.86	0.15	0.59	0.09	−0.65	0.12	−0.71	−0.11	−1.00	−0.33

corresponding to a perfect tetrahedron. In a similar way to what happened in mechanism I-8 the transition vector has also a quite low frequency value (around 350 cm^{-1}). The geometry parameters of the TS of mechanism I-6S are reflected in the natural atomic populations shown in Table 5. One can observe that the charges over H1, O2', and O1 present the maximum positive value, the minimum negative value, and the maximum negative value, respectively. This implies that there is a concentration of positive charge around O2' and a concentration of negative charge around O1 (oxyanion). In other words, it is the mechanism with the greatest zwitterionic character in the concerted TS, this fact being confirmed by the high dipole moment of this structure (11.67 D).

To get a deeper insight into mechanism I-6S, one has to consider the effect of the polarization induced by the solvent reaction field. In fact, if one computes the dipole moment of the I-6S TS in vacuo at the geometry optimized in solution (Figure 3), the dipole moment diminishes from 11.67 to 7.79 D, thus showing the large contribution of the polarization effect. Similar changes are found in the variation of the charges of the five atoms considered in Table 5. As it has already been mentioned, the calculated energies shown in Table 5 for the mechanisms in solution have been obtained by adding free energy of solvation to gas-phase potential energy surface. To estimate the value of the free energy of solvation of the TS, one has to subtract the E' value of the TS in solution from the value of E computed in vacuo with the geometry optimized in solution. This calculation leads to a stabilization of $43.1\text{ kcal mol}^{-1}$, coming, as usual, from an enthalpy term and an entropy term. Given that the formation of a zwitterion leads to a reorganization of the solvent, there will be a great contribution of the entropy term to the activation free energy. It is also worth mentioning that the mechanisms in the ribosome which are the most similar to I-6S are the I-6wf and I-6ff, in which the two additional molecules act as an oxanion hole. The comparison between these two mechanisms shows that the presence of solvent does not dramatically change the mechanism of the peptide release process.

■ DISCUSSION

A first point that deserves some discussion is the fact that the barriers presented in Table 1 are clearly overestimated, thus leading to rate constants much lower than the experimental ones.^{27,46} This overestimation, however, does not affect the main goal of our study, which, as indicated in the Introduction, is to compare the transition structures and the mechanisms of the two processes—peptide bond formation and peptide release—that take place in the same active center of the ribosome. One has to be aware that methodological limitations are inherent in quantum-mechanical studies of complex systems. The first limitation is due to the need to use a reduced model of the real system. In fact, Table 1 shows that the energy barriers decrease as far as additional molecules are included. However, the number of additional molecules is limited by the fact that they can interact with each other and

thus produce undesired artifacts. A second limitation is that the effect of environment in the chemical processes is not introduced in the catalyzed reaction. This implies that the system is allowed to be more flexible than it really is, since the constraints due to the physical environment are not taken into account. As it has been previously mentioned, the simplified model used in our calculations does not permit consideration of the real role played by the ribosome as an entropy trap (orienting and positioning substrates), this fact leading to a positive value of the ΔG of formation of the reactant complex. Moreover, the electrostatic embedding, due to the electrical field created by the enzyme, is poorly considered, since only oxanion holes have been introduced in some cases. Given the zwitterionic character of our TS, it may be expected that the effect of the electrostatic embedding can appreciably lower the energy barrier. Furthermore, the weaker nucleophilicity of water relative to the primary amine of an amino acid makes the release reaction more challenging and thus more dependent on sophisticated enzyme mechanisms.⁴⁶ The introduction of the surrounding effects (mechanical and electrical embedding) played by the ribosome would need hybrid QM/MM calculations, but this is quite difficult for our system. On one side, the MM methodology is not yet well developed for RNA systems.^{92,93} Furthermore, the calculation of free energy surfaces would require a semiempirical method able to accurately reproduce the ab initio results obtained in this work.

It is also worth discussing the position of the water molecules used in our model. X-ray studies with a resolution of $3\text{--}3.5\text{ \AA}$ ^{47–49} do not contain any information regarding water positions, including the important one that intervenes in the hydrolytic termination reaction. A crystal structure of release factor 2 bound to ribosome with an aminoacyl tRNA substrate analogue at the ribosomal P-site, obtained at 3.1 \AA resolution,⁵¹ together with previous biochemical and computational data,⁶⁵ suggests a model for how the ester bond between the peptidyl tRNA and the nascent peptide is hydrolyzed. Our Michaelis complex is in good agreement with this model. Regarding the other two water molecules, which interact with the oxanion or with both O2' and O3', we have used, as suggested by Trobro and Aqvist,⁶⁵ representative average structures of reactants and transition states, which are in good agreement with high-resolution ($2.3\text{--}2.7\text{ \AA}$) X-ray data for the active center of peptidyl transferase reaction.⁹⁰ This shows again that the peptide release process is much less known than the peptide bond formation reaction. At present, only medium resolution X-ray results of crystal structures mimicking reactant complexes⁵¹ or products^{47–49} are available. Higher resolution crystal structures of the ribosome with RF2 and transition state analogues would be required to elucidate the real mechanism.⁵¹

Let us analyze the results obtained for the 11 mechanisms we have considered. As it has been mentioned above, mechanism I-6 presents an energy barrier which is 5.8 kcal mol^{-1} lower than that of mechanism I-4, this fact implying that the substrate assisted catalysis favors the process. Our results are in good agreement with the experimental conclusions of previous

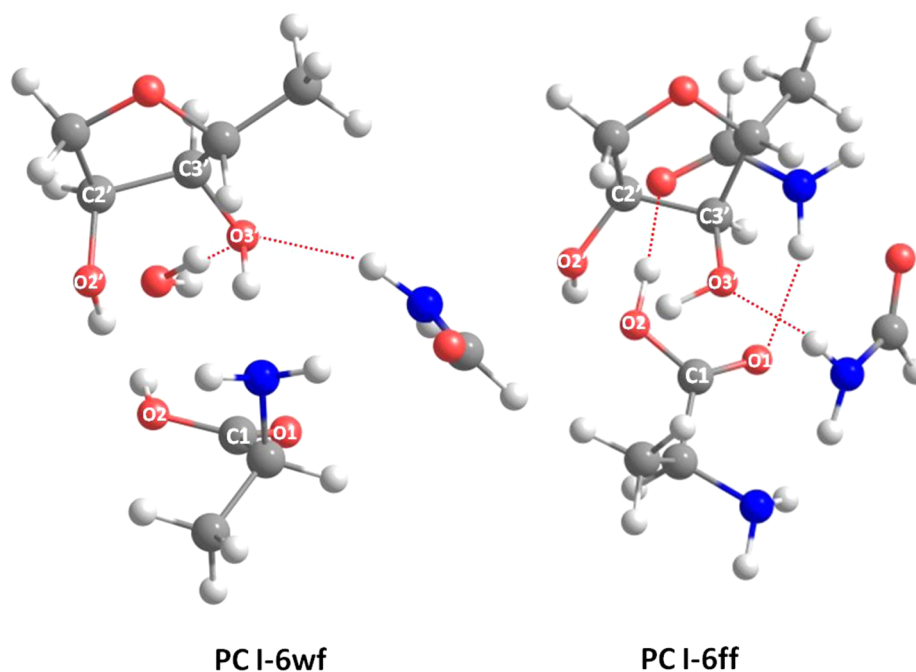


Figure 4. Geometries of the product complexes (PC) corresponding to mechanisms **I-6wf** and **I-6ff**.

studies^{57,59} about the important role played by the 2'-OH in the release reaction. On the other hand, in mechanisms **I-6f1** and **I-6f2**, the formamide molecule has been used to model the amide groups present in the main or in the lateral chain of the glutamine in the GGQ motif. The lack of catalytic effect in mechanism **I-6f1** (see Table 1) questions the suggestions of some experimental works^{45,48,49,52,53} about the role played by the amide group of the main chain. In contrast, our results indicate that in mechanism **I-6f2** the role of formamide is not only the orientation of the water molecule for the nucleophile attack, as suggested by some authors,^{1,12,45,47,50,51,53} but also the activation of this molecule. As one can observe in Table 1, the introduction of a water molecule in mechanisms **I-8**, **I-6w1**, and **I-6w2** does have a noticeable catalytic effect. In **I-8**, the water molecule intervenes in a cooperative hydrogen bond between O2' and O3', while in the other two mechanisms it plays the role of an oxyanion hole with respect to O1. In fact, several authors^{1,64,65} suggested that the catalytic role of the N-H group of the main chain is carried out through a water molecule. When, following the idea of Richter et al.,⁹⁴ both a water and a formamide molecule are introduced as an oxyanion hole (mechanism **I-6wf**), a good catalytic effect is also obtained. Finally, the introduction of two formamide molecules to represent the main and the lateral chain (mechanism **I-6ff**) leads to the lowest energy barrier. This is due to the fact that, apart from the hydrogen bond between the carbonyl oxygen atom of the formamide molecule and O2, the N-H group of the lateral chain and the amino group of the formamide representing the main chain play the role of an oxyanion hole. Mechanisms **I-6wf** and **I-6ff** confirm the proposal of Noller's group^{52,53} that the N-H of the main chain is hydrogen bonded to the oxyanion in the TS, while it is bonded to O3' in the product (see Figure 4). Regarding the mechanism in solution, it has already been mentioned that the charge over the oxyanion reaches its maximum in mechanism **I-6S**, the next values being those of mechanisms **I-6wf** and **I-6ff**.

As stated in the Introduction, one of the goals of this study is to compare the results obtained in this paper for the hydrolysis

reaction with those previously obtained by us⁷³ in the aminolysis process which takes place in the peptide bond formation at the same active center. In fact, both studies have been carried out with the same simplified model, the same density functional, the same basis set, and the same method for the introduction of the solvent. One point that deserves to be mentioned is the role played by the 2'-OH in the proton shuttle mechanism. In the present paper we have found that it does play an important role in the peptide release process, since mechanisms **I-6** and **I-6S** are more favorable than **I-4** and **I-4S**, respectively. On the contrary its role was not found in the peptide bond formation reaction, mechanism **I-4** being there more favorable than **I-6** and the TS of mechanism **I-6S** leading to a four-membered ring structure instead of the expected six-membered one. This different behavior is in excellent agreement with the recent experimental results of Strobel and Green's group⁵⁹ which show that the 2'-OH plays a quite different role in the mechanism of both processes, thus reconciling the conflict in the previous literature where some authors affirmed that the proton shuttle mechanism had a similar role in the peptide bond formation. Recent experimental studies^{95,96} have confirmed that there are mechanistic differences between aminolysis and hydrolysis.

Our calculations give support to these mechanistic differences. For the concerted peptide bond formation process (aminolysis), we found⁷³ that the nucleophilic attack of the N2 atom to the carboxylic C1 atom is accompanied by the transfer of a hydrogen atom to the O3' atom. Although the heterolytic breaking of the C1-O3' bond is quite advanced in the TS, the hydrogen transfer from N2 to O2' is only at an initial stage, in such a way that the transition structure has some ion-pair character. In fact, the reaction in solution could be assimilated to a S_N2 process between two neutral molecules, which is similar to the Mentschutkin reaction, although, in our case, the final products were also neutral since a proton was transferred from one fragment to the other in the second stage of the process. For the concerted peptide release reaction TS, in contrast, the hydrogen transfer from O2 to O2' is quite

advanced, the breaking of the C1–O3' carboxylic bond is at an initial stage, and the C1–O1 double bond has an important single bond character, especially in the presence of molecules acting as oxyanion holes. So, in this case, the C1 atom has a tetrahedral structure and the TS presents a zwitterionic character, especially in solution (see Figure 3 and Table 5). In a second stage of the process, the C1–O3' bond is broken, there is a proton transfer from O2 to O3', and the C1–O1 bond recovers its double bond character. The O2' atom is thus acting as a catalytic base in the hydrolysis reaction, but this role is not efficient in the aminolysis process given the high pK_a value of water when compared to the amine group. However this conclusion could be modified if our model took into account the effect of the electrical field created by the environment, this effect being able to change the pK_a of the nucleophile and the basicity of O2'.

Another mechanistic difference between both processes is that the zwitterionic intermediate suggested by some authors⁹⁰ for the peptide bond formation was really found at the very beginning of the reaction for the process in solution, the positive charge being localized over the amino group. The presence of a zwitterionic intermediate was not found when the reaction takes place in the ribosome, in good agreement with the experimental observation that the TS is scarcely stabilized by the presence of an oxyanion hole.⁹⁷ In the present paper, in contrast, the positive charge of the zwitterionic six-membered ring transition structures found for the hydrolysis reaction is concentrated over the sugar. Any attempt to localize a zwitterionic intermediate similar to the one found in the aminolysis process in solution failed.

CONCLUSIONS

From the results obtained in this paper for the concerted peptide release process we can conclude that the 2'-OH plays an important catalytic role and that the reaction takes place via a zwitterionic transition state, this TS being stabilized by the presence of oxyanion holes or by the solvent.

The comparison with our previous study⁷³ on the peptide bond formation shows that both processes proceed via two different mechanisms, in such a way that the TS of the aminolysis has an ion-pair instead of a zwitterionic character. This difference is mainly due to the higher acidity of water with respect to the amino group. As a direct consequence, the proton transfer from O2 to O2' in the hydrolysis TS is much more advanced than the proton transfer from N2 to O2' in the aminolysis TS. So, despite the limitations of the model we have used, we can conclude that there is also a catalytic promiscuity at the peptidyl transferase center (PTC) of the ribosome.

ASSOCIATED CONTENT

Supporting Information

Complete refs 41, 42, 86, and 94, Cartesian coordinates of transition state structures, and absolute energies (in hartrees) for all the optimized structures. This material is available free of charge via the Internet at <http://pubs.acs.org>.

AUTHOR INFORMATION

Notes

The authors declare no competing financial interest.

ACKNOWLEDGMENTS

Financial support from Ministerio de Economía y Competitividad (through Grants CTQ2011-24847 and CTQ2010-15408) and Generalitat de Catalunya (through Grants SGR2009-733 and XRQTC) and allowance of computer resources from the CESCA supercomputing center are gratefully acknowledged.

REFERENCES

- (1) Leung, E. K. Y.; Suslov, N.; Tuttle, N.; Sengupta, R.; Piccirilli, J. A. The Mechanism of Peptidyl Transfer Catalysis by the Ribosome. *Annu. Rev. Biochem.* **2011**, *80*, 527–555.
- (2) Youngman, E. M.; McDonald, M. E.; Green, R. Peptide Release on the Ribosome: Mechanism and Implications for Translational Control. *Annu. Rev. Microbiol.* **2008**, *62*, 353–373.
- (3) Schmeing, T. M.; Huang, K. S.; Strobel, S. A.; Steitz, T. A. An Induced-Fit Mechanism to Promote Peptide Bond Formation and Exclude Hydrolysis of Peptidyl-tRNA. *Nature* **2005**, *438*, 520–524.
- (4) Simonovic, M.; Steitz, T. A. Peptidyl-CCA Deacylation on the Ribosome Promoted by Induced Fit and the O3'-Hydroxyl Group of A76 of the Unacylated A-Site tRNA. *RNA* **2008**, *14*, 2372–2378.
- (5) O'Brien, P. J.; Herschlag, D. Catalytic Promiscuity and the Evolution of New Enzymatic Activities. *Chem. Biol.* **1999**, *6*, R91–R105.
- (6) Copley, S. D. Enzymes with Extra Talents: Moonlighting Functions and Catalytic Promiscuity. *Curr. Opin. Chem. Biol.* **2003**, *7*, 265–272.
- (7) Khersonsky, O.; Roodveldt, C.; Tawfik, D. S. Enzyme Promiscuity: Evolutionary and Mechanistic Aspects. *Curr. Opin. Chem. Biol.* **2006**, *10*, 498–508.
- (8) Toscano, M. D.; Woycechowsky, K. J.; Hilvert, D. Minimalist Active-Site Redesign: Teaching Old Enzymes New Tricks. *Angew. Chem., Int. Ed.* **2007**, *46*, 3212–3236.
- (9) Khersonsky, O.; Tawfik, D. S. Enzyme Promiscuity: a Mechanistic and Evolutionary Perspective. *Annu. Rev. Biochem.* **2010**, *79*, 471–505.
- (10) Capecchi, M. R. Polypeptide Chain Termination in Vitro: Isolation of a Release Factor. *Biochemistry* **1967**, *58*, 1144–1151.
- (11) Ito, K.; Uno, M.; Nakamura, Y. A Tripeptide 'Anticodon' Deciphers Stop Codons in Messenger RNA. *Nature* **2000**, *403*, 680–684.
- (12) Song, H.; Mugnier, P.; Das, A. K.; Webb, H. M.; Evans, D. R.; Tuite, M. F.; Hemmings, B. A.; Barford, D. The Crystal Structure of Human Eukaryotic Release Factor eRF1. Mechanism of Stop Codon Recognition and Peptidyl-tRNA Hydrolysis. *Cell* **2000**, *100*, 311–321.
- (13) Nakamura, Y.; Ito, K. A Tripeptide Discriminator for Stop Codon Recognition. *FEBS Lett.* **2002**, *514*, 30–33.
- (14) Uno, M.; Ito, K.; Nakamura, Y. Polypeptide Release at Sense and Noncognate Stop Codons by Localized Charge-Exchange Alterations in Translational Release Factors. *Proc. Natl. Acad. Sci. U.S.A.* **2002**, *99*, 1819–1824.
- (15) Chavatte, L.; Seit-Nebi, A.; Dubovaya, V.; Favre, A. The Invariant Uridine of Stop Codon Contacts the Conserved NIKSR Loop of Human eRF1 in the Ribosome. *EMBO J.* **2002**, *21*, 5302–5311.
- (16) Kisselev, L.; Ehrenberg, M.; Frolova, L. Termination of Translation: Interplay of mRNA, rRNAs and Release Factors? *EMBO J.* **2003**, *22*, 175–182.
- (17) Youngman, E. M.; He, S. L.; Nikstad, L. J.; Green, R. Stop Codon Recognition by Release Factors Induces Structural Rearrangement of the Ribosomal Decoding Center that is Productive for Peptide Release. *Mol. Cell* **2007**, *28*, 533–543.
- (18) Field, A.; Hetrick, B.; Matthew, M.; Joseph, S. Histidine 197 in Release Factor 1 is Essential for A Site Binding and Peptide Release. *Biochemistry* **2010**, *49*, 9385–9390.
- (19) Chrzanowska-Lightowlers, Z. M. A.; Pajak, A.; Lightowlers, R. N. Termination of Protein Synthesis in Mammalian Mitochondria. *J. Biol. Chem.* **2011**, *286*, 34479–34485.

- (20) Frolova, L. Y.; Tsivkovskii, R. Y.; Sivolobova, G. F.; Oparina, N. Y.; Serpinsky, O. I.; Blinov, V. M.; Tatkov, S. I.; Kisselev, L. L. Mutations in the Highly Conserved GGQ Motif of Class 1 Polypeptide Release Factors Abolish Ability of Human eRF1 to Trigger Peptidyl-tRNA Hydrolysis. *RNA* **1999**, *5*, 1014–1020.
- (21) Dinçbas-Renqvist, V.; Engström, A.; Mora, L.; Heurgué-Hamard, V.; Buckingham, R.; Ehrenberg, M. A Post-Translational Modification in the GGQ Motif of RF2 from *Escherichia coli* Stimulates Termination of Translation. *EMBO J.* **2000**, *19*, 6900–6907.
- (22) Seit-Nebi, A.; Frolova, L.; Justesen, J.; Kisselev, L. Class-1 Translation Termination Factors: Invariant GGQ Minidomain is Essential for Release Activity and Ribosome Binding but not for Stop Codon Recognition. *Nucleic Acids Res.* **2001**, *29*, 3982–3987.
- (23) Heurgué-Hamard, V.; Champ, S.; Mora, L.; Merkoulouva-Rainon, T.; Kisselev, L. L.; Buckingham, R. H. The Glutamine Residue of the Conserved GGQ Motif in *Saccharomyces cerevisiae* Release Factor eRF1 is Methylated by the Product of the YDR140w Gene. *J. Biol. Chem.* **2005**, *280*, 2439–2445.
- (24) Graille, M.; Heurgué-Hamard, V.; Champ, S.; Mora, L.; Scrima, N.; Ulryck, N.; Tilbeurgh, H. v.; Buckingham, R. H. Molecular Basis for Bacterial Class I Release Factor Methylation by PrmC. *Mol. Cell* **2005**, *20*, 917–927.
- (25) Polevoda, B.; Span, L.; Sherman, F. The Yeast Translation Release Factors Mrf1p and Sup45p (eRF1) are Methylated, respectively, by the Methyltransferases Mtq1p and Mtq2p. *J. Biol. Chem.* **2006**, *281*, 2562–2571.
- (26) Mora, L.; Heurgué-Hamard, V.; Zamaroczy, M.; Kervestin, S.; Buckingham, R. H. Methylation of Bacterial Release Factors RF1 and RF2 is Required for Normal Translation Termination *In Vivo*. *J. Biol. Chem.* **2007**, *282*, 35638–35645.
- (27) Zavialov, A. V.; Mora, L.; Buckingham, R. H.; Ehrenberg, M. Release of Peptide Promoted by the GGQ Motif of Class 1 Release Factors Regulates the GTPase Activity of RF3. *Mol. Cell* **2002**, *10*, 789–798.
- (28) Rawat, U. B. S.; Zavialov, A. V.; Sengupta, J.; Valle, M.; Grassucci, R. A.; Linde, J.; Vestergaard, B.; Ehrenberg, M.; Frank, J. A Cryo-Electron Microscopic Study of Ribosome-Bound Termination Factor RF2. *Nature* **2003**, *421*, 87–90.
- (29) Klaholz, B. P.; Pape, T.; Zavialov, A. V.; Myasnikov, A. G.; Orlova, E. V.; Vestergaard, B.; Ehrenberg, M.; Heel, M. v. Structure of the *Escherichia coli* Ribosomal Termination Complex with Release Factor 2. *Nature* **2003**, *421*, 90–94.
- (30) Mora, L.; Heurgué-Hamard, V.; Champ, S.; Ehrenberg, M.; Kisselev, L. L.; Buckingham, R. H. The Essential Role of the Invariant GGQ Motif in the Function and Stability *In Vivo* of Bacterial Release Factors RF1 and RF2. *Mol. Microbiol.* **2003**, *47*, 267–275.
- (31) Ma, B.; Nussinov, R. Release Factors eRF1 and RF2. A Universal Mechanism Controls the Large Conformational Changes. *J. Biol. Chem.* **2004**, *279*, 53875–53885.
- (32) Shin, D. H.; Brandsen, J.; Jancarik, J.; Yokota, H.; Kim, R.; Kim, S.-H. Structural Analyses of Peptide Release Factor 1 from *Thermotoga maritima* Reveal Domain Flexibility Required for its Interaction with the Ribosome. *J. Mol. Biol.* **2004**, *341*, 227–239.
- (33) Petry, S.; Brodersen, D. E.; Murphy, F. V., IV; Dunham, C. M.; Selmer, M.; Tarry, M. J.; Kelley, A. C.; Ramakrishnan, V. Crystal Structures of the Ribosome in Complex with Release Factors RF1 and RF2 Bound to a Cognate Stop Codon. *Cell* **2005**, *123*, 1255–1266.
- (34) Rawat, U.; Gao, H.; Zavialov, A.; Gursky, R.; Ehrenberg, M.; Frank, J. Interactions of the Release Factor RF1 with the Ribosome as Revealed by Cryo-EM. *J. Mol. Biol.* **2006**, *357*, 1144–1153.
- (35) Ivanova, E. V.; Kolosov, P. M.; Birdsall, B.; Kelly, G.; Pastore, A.; Kisselev, L. L.; Polshakov, V. I. Eukaryotic Class 1 Translation Termination Factor eRF1. The NMR Structure and Dynamics of the Middle Domain Involved in Triggering Ribosome-Dependent Peptidyl-tRNA Hydrolysis. *FEBS J.* **2007**, *274*, 4223–4237.
- (36) Vestergaard, B.; Sanyal, S.; Roessie, M.; Mora, L.; Buckingham, R. H.; Kastrop, J. S.; Gajhede, M.; Svergun, D. I.; Ehrenberg, M. The SAXS Solution Structure of RF1 Differs from its Crystal Structure and is Similar to its Ribosome Bound Cryo-EM Structure. *Mol. Cell* **2005**, *20*, 929–938.
- (37) Zoldák, G.; Redecke, L.; Svergun, D. I.; Konarev, P. V.; Voertler, C. S.; Dobbek, H.; Sedláč, E.; Sprinzl, M. Release Factors 2 from *Escherichia coli* and *Thermus thermophilus*: Structural, Spectroscopic and Microcalorimetric Studies. *Nucleic Acids Res.* **2007**, *35*, 1343–1353.
- (38) Salas-Marco, J.; Bedwell, D. M. GTP Hydrolysis by eRF3 Facilitates Stop Codon Decoding during Eukaryotic Translation Termination. *Mol. Cell. Biol.* **2004**, *24*, 7769–7778.
- (39) Alkalaeva, E. Z.; Pisarev, A. V.; Frolova, L. Y.; Kisselev, L. L.; Pestova, T. V. In Vitro Reconstitution of Eukaryotic Translation Reveals Cooperativity between Release Factors eRF1 and eRF3. *Cell* **2006**, *125*, 1125–1136.
- (40) Dubovaya, V. I.; Kolosov, P. L.; Alkalaeva, E. Z.; Frolova, L. Y.; Kisselev, L. L. Influence of Individual Domains of the Translation Termination Factor eRF1 on Induction of the GTPase Activity of the Translation Termination Factor eRF3. *Mol. Biol.* **2006**, *40*, 270–275.
- (41) Gao, H.; Zhou, Z.; Rawat, U.; Huang, C.; Bouakaz, L.; Wang, C.; Cheng, Z.; Liu, Y.; Zavialov, A.; Gursky, R.; et al. RF3 Induces Ribosomal Conformational Changes Responsible for Dissociation of Class I Release Factors. *Cell* **2007**, *129*, 929–941.
- (42) Cheng, Z.; Saito, K.; Pisarev, A. V.; Wada, M.; Pisareva, V. P.; Pestova, T. V.; Gajda, M.; Round, A.; Kong, C.; Lim, M.; et al. Structural Insights into eRF3 and Stop Codon Recognition by eRF1. *Genes Dev.* **2009**, *23*, 1106–1118.
- (43) Zaher, H. S.; Green, R. A Primary Role for Release Factor 3 in Quality Control during Translation Elongation in *Escherichia coli*. *Cell* **2011**, *147*, 396–408.
- (44) Vestergaard, B.; Van, L. B.; Andersen, G. R.; Nyborg, J.; Buckingham, R. H.; Kjeldgaard, M. Bacterial Polypeptide Release Factor RF2 is Structurally Distinct from Eukaryotic eRF1. *Mol. Cell* **2001**, *8*, 1375–1382.
- (45) Dunkle, J. A.; Cate, J. H. D. Ribosome Structure and Dynamics during Translocation and Termination. *Annu. Rev. Biophys.* **2010**, *39*, 227–244.
- (46) Shaw, J. J.; Green, R. Two Distinct Components of Release Factor Function Uncovered by Nucleophile Partitioning Analysis. *Mol. Cell* **2007**, *28*, 458–467.
- (47) Weixlbaumer, A.; Jin, H.; Neubauer, C.; Voorhees, R. M.; Petry, S.; Kelley, A. C.; Ramakrishnan, V. Insights into Translational Termination from the Structure of RF2 bound to the Ribosome. *Science* **2008**, *322*, 953–956.
- (48) Laurberg, M.; Asahara, H.; Korostelev, A.; Zhu, J.; Trakhanov, S.; Noller, H. Structural Basis for Translation Termination on the 70S Ribosome. *Nature* **2008**, *454*, 852–857.
- (49) Korostelev, A.; Asahara, H.; Lancaster, L.; Laurberg, M.; Hirschi, A.; Zhu, J.; Trakhanov, S.; Scott, W. G.; Noller, H. F. Crystal Structure of a Translation Termination Complex Formed with Release Factor RF2. *Proc. Natl. Acad. Sci. U.S.A.* **2008**, *105*, 19684–19689.
- (50) Loh, P. G.; Song, H. Structural and Mechanistic Insights into Translation Termination. *Curr. Opin. Struct. Biol.* **2010**, *20*, 98–103.
- (51) Jin, H.; Kelley, A. C.; Loakes, D.; Ramakrishnan, V. Structure of the 70S Ribosome Bound to Release Factor 2 and a Substrate Analog Provides Insights into Catalysis of Peptide Release. *Proc. Natl. Acad. Sci. U.S.A.* **2010**, *107*, 8593–8598.
- (52) Korostelev, A.; Zhu, J.; Asahara, H.; Noller, H. F. Recognition of the Amber UAG Stop Codon by Release Factor RF1. *EMBO J.* **2010**, *29*, 2577–2585.
- (53) Klaholz, B. P. Molecular Recognition and Catalysis in Translation Termination Complexes. *Trends Biochem. Sci.* **2011**, *36*, 282–292.
- (54) Polacek, N.; Gomez, M. J.; Ito, K.; Xiong, L.; Nakamura, Y.; Mankin, A. The Critical Role of the Universally Conserved A2602 of 23S Ribosomal RNA in the Release of the Nascent Peptide during Translation Termination. *Mol. Cell* **2003**, *11*, 103–112.
- (55) Youngman, E. M.; Brunel, J. L.; Kochaniak, A. B.; Green, R. The Active Site of the Ribosome is Composed of two Layers of Conserved

Nucleotides with Distinct Roles in Peptide Bond Formation and Peptide Release. *Cell* **2004**, *117*, 589–599.

(56) Amort, M.; Wotzel, B.; Bakowska-Zywicka, K.; Erlacher, M. D.; Micura, R.; Polacek, N. An Intact Ribose Moiety at A2602 of 23S rRNA is Key to Trigger Peptidyl-tRNA Hydrolysis during Translation Termination. *Nucleic Acids Res.* **2007**, *35*, 5130–5140.

(57) Brunelle, J. L.; Shaw, J. J.; Youngman, E. M.; Green, R. Peptide Release on the Ribosome Depends Critically on the 2'-OH of the Peptidyl-tRNA Substrate. *RNA* **2008**, *14*, 1526–1531.

(58) Weinger, J. S.; Parnell, K. M.; Dörner, S.; Green, R.; Strobel, S. A. Substrate-Assisted Catalysis of Peptide Bond Formation by the Ribosome. *Nat. Struct. Mol. Biol.* **2004**, *11*, 1101–1106.

(59) Zaher, H. S.; Shaw, J. J.; Strobel, S. A.; Green, R. The 2'-OH Group of the Peptidyl-tRNA Stabilizes an Active Conformation of the Ribosomal PTC. *EMBO J.* **2011**, *30*, 2445–2453.

(60) Trobro, S.; Aqvist, J. Mechanism of Peptide Bond Synthesis on the Ribosome. *Proc. Natl. Acad. Sci. U.S.A.* **2005**, *102*, 12395–12400.

(61) Trobro, S.; Aqvist, J. Analysis of Predictions for the Catalytic Mechanism of Ribosomal Peptidyl Transfer. *Biochemistry* **2006**, *45*, 7049–7056.

(62) Trobro, S.; Aqvist, J. Role of Ribosomal Protein L27 in Peptidyl Transfer. *Biochemistry* **2008**, *47*, 4898–4906.

(63) Warshel, A. *Computer Modeling of Chemical Reactions in Enzymes and Solutions*; John Wiley & Sons: New York, 1991.

(64) Trobro, S.; Aqvist, J. A Model for how Ribosomal Release Factors Induce Peptidyl-tRNA Cleavage in Termination of Protein Synthesis. *Mol. Cell* **2007**, *27*, 758–766.

(65) Trobro, S.; Aqvist, J. Mechanism of the Translation Termination Reaction on the Ribosome. *Biochemistry* **2009**, *48*, 11296–11303.

(66) Das, G. K.; Bhattacharyya, D.; Burma, D. P. A Possible Mechanism of Peptide Bond Formation on Ribosome without Mediation of Peptidyl Transferase. *J. Theor. Biol.* **1999**, *200*, 193–205.

(67) Suárez, D.; Merz, K. M. Quantum Chemical Study of Ester Aminolysis Catalyzed by a Single Adenine: a Reference Reaction for the Ribosomal Peptide Synthesis. *J. Am. Chem. Soc.* **2001**, *123*, 7687–7690.

(68) Gindulyte, A.; Bashan, A.; Agmon, I.; Massa, L.; Yonath, A.; Karle, J. The Transition State for Formation of the Peptide Bond in the Ribosome. *Proc. Natl. Acad. Sci. U.S.A.* **2006**, *103*, 13327–13332.

(69) Massa, L.; Matta, C. F.; Yonath, A.; Karle, J. Quantum Transition States for Peptide Bond Formation in the Ribosome. In *Quantum Biochemistry*; Matta, C. F., Ed.; Wiley-VCH Verlag: Weinheim, 2010; pp 501–515.

(70) Thirumoorthy, K.; Nandi, N. Role of Chirality of the Sugar Ring in the Ribosomal Peptide Synthesis. *J. Phys. Chem. B* **2008**, *112*, 9187–9195.

(71) Wallin, G.; Aqvist, J. The Transition State for Peptide Bond Formation Reveals the Ribosome as a Water Trap. *Proc. Natl. Acad. Sci. U.S.A.* **2010**, *107*, 1888–1893.

(72) Wang, Q.; Gao, J.; Liu, Y.; Liu, C. Validating a New Proton Shuttle Reaction Pathway for Formation of the Peptide Bond in Ribosomes: a Theoretical Investigation. *Chem. Phys. Lett.* **2010**, *501*, 113–117.

(73) Acosta-Silva, C.; Bertran, J.; Branchadell, V.; Oliva, A. Quantum-Mechanical Study on the Mechanism of Peptide Bond Formation in the Ribosome. *J. Am. Chem. Soc.* **2012**, *134*, 5817–5831.

(74) Tantillo, D. J.; Chen, J.; Houk, K. N. Theozymes and Compuzymes: Theoretical Models for Biological Catalysis. *Curr. Opin. Chem. Biol.* **1998**, *2*, 743–750.

(75) DeChancie, J.; Clemente, F. R.; Smith, A. J. T.; Gunaydin, H.; Zhao, Y.-L.; Zhang, X.; Houk, K. N. How Similar are Enzyme Active Site Geometries Derived from Quantum Mechanical Theozymes to Crystal Structures of Enzyme-Inhibitor Complexes? Implications for Enzyme Design. *Protein Sci.* **2007**, *16*, 1851–1866.

(76) Zhang, X.; DeChancie, J.; Gunaydin, H.; Chowdry, A. B.; Clemente, F. R.; Smith, A. J. T.; Handel, T. M.; Houk, K. N. Quantum Mechanical Design of Enzyme Active Sites. *J. Org. Chem.* **2008**, *73*, 889–899.

(77) Hratchian, H. P.; Schlegel, H. B. Accurate Reaction Paths Using a Hessian Based Predictor-Corrector Integrator. *J. Chem. Phys.* **2004**, *120*, 9918–9925.

(78) Zhao, Y.; Truhlar, D. G. The M06 Suite of Density Functionals for Main Group Thermochemistry, Thermochemical Kinetics, Non Covalent Interactions, Excited States and Transition Elements: Two New Functionals and Systematic Testing of Four M06-Class Functionals and 12 other Functionals. *Theor. Chem. Acc.* **2008**, *120*, 215–241.

(79) Zhao, Y.; Truhlar, D. G. Density Functionals with Broad Applicability in Chemistry. *Acc. Chem. Res.* **2008**, *41*, 157–167.

(80) Papajak, E.; Leverentz, H. R.; Zheng, J.; Truhlar, D. G. Efficient Diffuse Basis Sets: cc-pVxZ+ and maug-cc-pVxZ. *J. Chem. Theory Comput.* **2009**, *5*, 1197–1202.

(81) Papajak, E.; Truhlar, D. G. Efficient Diffuse Basis Sets for Density Functional Theory. *J. Chem. Theory Comput.* **2010**, *6*, 597–601.

(82) Papajak, E.; Truhlar, D. G. Convergent Partially Augmented Basis Sets for post-Hartree-Fock Calculations of Molecular Properties and Reaction Barriers Heights. *J. Chem. Theory Comput.* **2011**, *7*, 10–18.

(83) Marenich, A. V.; Cramer, C. J.; Truhlar, D. G. Universal Solvation Model Based on Solute Electron Density and on a Continuum Model of the Solvent Defined by the Bulk Dielectric Constant and Atomic Surface Tensions. *J. Phys. Chem. B* **2009**, *113*, 6378–6396.

(84) Marenich, A. V.; Olson, R. M.; Kelly, C. P.; Cramer, C. J.; Truhlar, D. G. Self-Consistent Reaction Field Model for Aqueous and Nonaqueous Solutions Based on Accurate Polarized Partial Charges. *J. Chem. Theory Comput.* **2007**, *3*, 2011–2033.

(85) Mc Quarrie, D. A. *Statistical mechanics*; Harper & Row: New York, 1986.

(86) Frisch, M. J.; Trucks, G. W.; Schlegel, H. B.; Scuseria, G. E.; Robb, M. A.; Cheeseman, J. R.; Scalmani, G.; Barone, V.; Mennucci, B.; Petersson, G. A. et al.; *Gaussian 09, Revision B.01*; Gaussian, Inc.: Wallingford, CT, 2009.

(87) Reed, A. E.; Curtiss, L. A.; Weinhold, F. Intermolecular Interactions from a Natural Bond Orbital, Donor-Acceptor Viewpoint. *Chem. Rev.* **1988**, *88*, 899–926.

(88) Page, M. I.; Jencks, W. P. Entropic Contributions to Rate Accelerations in Enzymic and Intramolecular Reactions and the Chelate Effect. *Proc. Natl. Acad. Sci. U.S.A.* **1971**, *68*, 1678–1683.

(89) Wiberg, K. A. Application of the Pople-Santry-Segal CNDO Method to the Cyclopropylcarbinyl and Cyclobutyl Cation and to Bicyclobutane. *Tetrahedron* **1968**, *24*, 1083–1096.

(90) Schmeing, T. M.; Huang, K. S.; Kitchen, D. E.; Strobel, S. A.; Steitz, T. A. Structural Insights into the Roles of Water and the 2'-Hydroxyl of the P Site tRNA in the Peptidyl Transferase Reaction. *Mol. Cell* **2005**, *20*, 437–448.

(91) Kim, Y.; Mohrig, J. R.; Truhlar, D. G. Free-Energy Surfaces for Liquid-Phase Reactions and their Use to Study the Border between Concerted and Nonconcerted α,β -Elimination Reactions of Esters and Thioesters. *J. Am. Chem. Soc.* **2010**, *132*, 11071–11082.

(92) Ditzler, M. A.; Otyepka, M.; Sponer, J.; Walter, N. G. Molecular Dynamics and Quantum Mechanics of RNA: Conformational and Chemical Change we Can Believe. *Acc. Chem. Res.* **2010**, *43*, 40–47.

(93) Tubbs, J. D.; Condon, D. E.; Kennedy, S. D.; Hauser, M.; Bevilacqua, P. C.; Turner, D. H. The Nuclear Magnetic Resonance of CCCC RNA Reveals a Right-Handed Helix, and Revised Parameters for AMBER Force Field Torsions Improve Structural Predictions from Molecular Dynamics. *Biochemistry* **2013**, *52*, 996–1010.

(94) Richter, F.; Blomberg, R.; Khare, S. D.; Kiss, G.; Kuzin, A. P.; Smith, A. J. T.; Gallaher, J.; Pianowski, Z.; Helgeson, R. C.; Grjasnow, A.; et al. Computational Design of Catalytic Dyads and Oxyanion Holes for Ester Hydrolysis. *J. Am. Chem. Soc.* **2012**, *134*, 16197–16206.

(95) Hiller, D. A.; Zhong, M.; Singh, V.; Strobel, S. A. Transition States of Uncatalyzed Hydrolysis and Aminolysis Reactions of a

Ribosomal P-Site Substrate Determined by Kinetic Isotope Effects. *Biochemistry* **2010**, 49, 3868–3878.

(96) Kuhlenkoetter, S.; Wintermeyer, W.; Rodnina, M. V. Different Substrate-Dependent Transition States in the Active Site of the Ribosome. *Nature* **2011**, 476, 351–355.

(97) Carrasco, N.; Hiller, D. A.; Strobel, S. A. Minimal Transition State Charge Stabilization of the Oxyanion during Peptide Bond Formation by the Ribosome. *Biochemistry* **2011**, 50, 10491–10498.